

ELECTROMAGNETIC ENERGY HARVESTER WITH MECHANICAL AMPLIFIER FOR TRANSLATIONAL KINETIC

M. Černý*, M. Dzurilla**, M. Musil***

Abstract: *This paper deals with the design and construction of a mechanical amplifier coupled to an electromagnetic energy harvester to generate power from low-amplitude (± 2 mm) and low-frequency (≤ 8 Hz). Design and simulation guidance of magnetic flux to achieve an effective changes of the polarity.*

Keywords: Harvester, Amplifier, Electromagnetism, Mechanism, Guidance.

1. Introduction

Today's level of minimization allows many devices to be used in places that were unthinkable until now. Particularly, given the wireless data transmission, sensors are limited by the necessity of electric power supply. When using the cable system to power the devices, the advantages of wireless communication are considerably reduced. Using batteries is not the best solution because of their life expectancy and limited working conditions. To push the boundaries of the possibilities for technical control and management, the scientists have recently been exploring new alternatives based on the inexhaustible energy sources in the close distance around the powered system.

One of the most effective alternative ways to supply power to consumer electronic devices seems to be the exploitation of the surrounding vibrations. However, kinetic parameters of standard environment, including human movement, vibration of bridges, buildings and many devices and machines, are low-frequency. To solve this problem, many solutions were designed, such as exploitation of resonance oscillation (Sardini et al., 2011), mechanical frequency, or rotating movement with eccentric mass. Performance of many of these systems goes down out of the range of appropriate conditions, whenever there are big static displacement, non-periodic vibrations and low amplitude. The range is usually narrow, which is a huge disadvantage. The opposite approach to this solution is "direct force", where vibrations are transmitted only by transfer multiplying amplitude and frequency (Shahosseini et al., 2014). Although these solutions tend to create less energy compared to resonance harvesters, they have the advantage of a wider excitation band. Their disadvantage, however, is that they might not be applicable everywhere, especially, as far as vehicles are concerned. That is why this paper is focused on harvester with mechanical amplifier.

2. Harvester design

The core of the phenomenon explored is an oscillating body which is able to amplify small amplitude $0.325R$ -times thanks to an amplifying gear connected to a coil on a crank. System of magnets in the trajectory of the coil multiplies the frequency 4 times, given a maximum oscillation. Oscillating body with mass " m " with a crest secured on a base is shown in Fig. 1. There is a pendulum connected to the base with a mass " m_2 " with its center of gravity in a position " R " from the rotation axis, with a gear of inertia " I " and a gear radius " r ". The gear ratio is $1 \text{ mm} = 18^\circ$.

* Ing. Michal Černý: Faculty of Mechanical Engineering STU in Bratislava; Námetie Slobody 17; 812 31 Bratislava 1; SK, michal.cerny@stuba.sk

** Ing. Michal Dzurilla: Faculty of Mechanical Engineering STU in Bratislava; Námetie Slobody 17; 812 31 Bratislava 1; SK, michal.dzurilla@stuba.sk

*** Prof. Ing. Miloš Musil, CSc.: Faculty of Mechanical Engineering STU in Bratislava; Námetie Slobody 17; 812 31 Bratislava 1; SK, milos.musil@stuba.sk

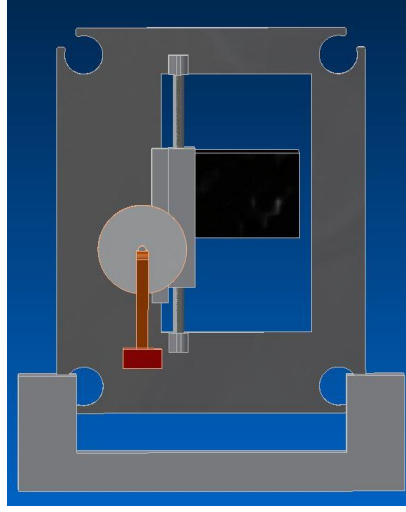


Fig. 1: Simplified model of mechanism.

Basic description of dynamic mechanism:

$$x = r \sin \varphi \rightarrow \dot{x} = \dot{\varphi} r \cos \varphi \quad (1)$$

$$E_k = \frac{1}{2} m \dot{x}^2 + \frac{1}{2} I \dot{\varphi}^2 = \frac{1}{2} m r^2 \dot{\varphi}^2 \cos^2 \varphi + \frac{1}{2} I \dot{\varphi}^2 \quad (2)$$

$$E_p = \frac{1}{2} m_2 g R (1 - \cos \varphi) \quad (3)$$

$$\frac{d}{dt} \left(\frac{\partial E_k}{\partial \dot{\varphi}} \right) - \frac{\partial E_k}{\partial \varphi} + \frac{\partial E_p}{\partial \varphi} + \frac{\partial D}{\partial \dot{\varphi}} = Q_j \quad (4)$$

$$\frac{\partial E_k}{\partial \dot{\varphi}} = \frac{\partial}{\partial \dot{\varphi}} \left(\frac{1}{2} m r^2 \dot{\varphi}^2 \cos^2 \varphi + \frac{1}{2} I \dot{\varphi}^2 \right) = m r^2 \dot{\varphi} \cos^2 \varphi + I \dot{\varphi} \quad (5)$$

$$\frac{d}{dt} \left(\frac{\partial E_k}{\partial \dot{\varphi}} \right) = m r^2 \ddot{\varphi} \cos^2 \varphi - 2 m r^2 \dot{\varphi} \cos \varphi \sin \varphi + I \ddot{\varphi} = m r^2 (\ddot{\varphi} \cos^2 \varphi - \dot{\varphi} \sin(2\varphi)) + I \ddot{\varphi} \quad (6)$$

$$\frac{\partial E_k}{\partial \varphi} = \frac{\partial}{\partial \varphi} \left(\frac{1}{2} 2 m r^2 \dot{\varphi}^2 \cos^2 \varphi + \frac{1}{2} I \dot{\varphi}^2 \right) = - 2 m r^2 \dot{\varphi}^2 \cos \varphi \sin \varphi = - \frac{1}{2} m r^2 \dot{\varphi}^2 \sin(2\varphi) \quad (7)$$

$$\frac{\partial E_p}{\partial \varphi} = + \frac{1}{2} m_2 g R \sin \varphi \quad (8)$$

$$m r^2 (\ddot{\varphi} \cos^2 \varphi - \dot{\varphi} \sin 2\varphi) + I \ddot{\varphi} + \frac{1}{2} m r^2 \dot{\varphi}^2 \sin(2\varphi) + \frac{1}{2} m_2 g R \sin \varphi = 0 \quad (9)$$

$$\ddot{\varphi} [m r^2 \cos^2 \varphi + I] + \dot{\varphi}^2 \frac{1}{2} m r^2 \sin 2\varphi - \dot{\varphi} m r^2 \sin 2\varphi + \frac{1}{2} m_2 g R \sin \varphi = 0 \quad (10)$$

As shown in Fig. 2, pairs of the magnets are located on the both sides of the corridor track. Corridor track is an air gap, where the coil is moving. Each pair of magnets has same orientation. Every pair is oppositely oriented as its nearby pair. For more effective guidance of magnetic flux is using steel slabs with higher-order value permeability than air. Description of Fig. 2, red: steel material, blue: magnets, orange: Polylactic acid (PLA)

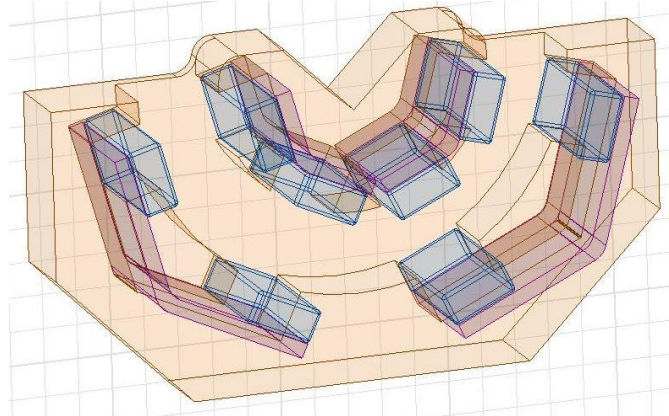


Fig. 2: Corridor for the coil.

Field distribution of magnetic induction in the air gap is the most important parameter, which decides the parameter of the generator. In particular the dependence of magnetic induction, which passes through the coil, thus the size if the induced voltage.

Between the magnets is the moving coil. The exact value depends on specific constructive solution. Due to the construction and location of the permanent magnets, the magnetic induction is not constant. Its assembly, they used method of finite element method and magneto-static analysis. A shown in Fig. 3, we can see magnetic circuit and distribution of magnetic induction.

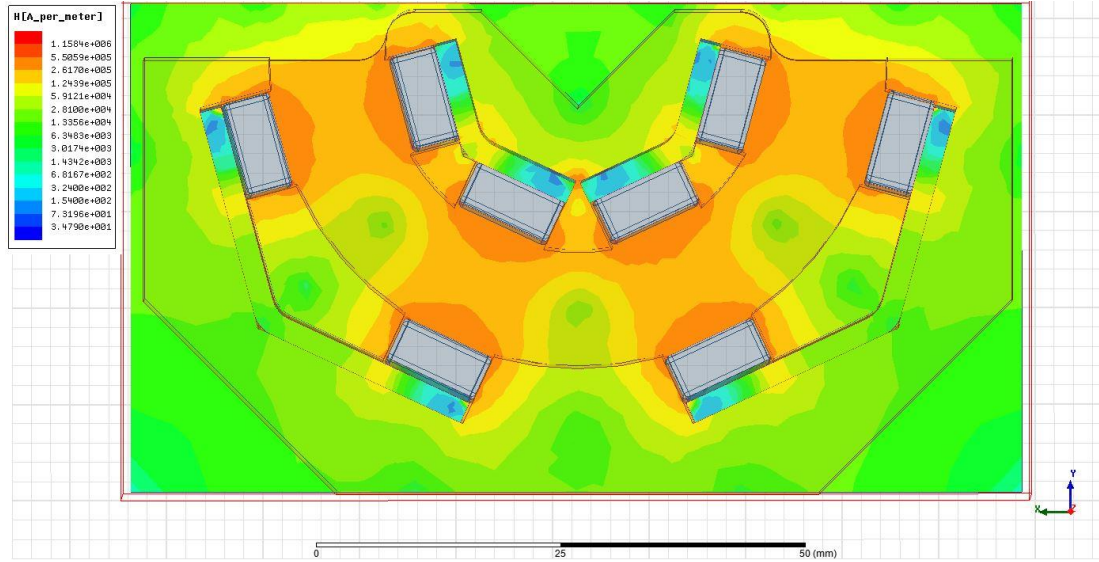


Fig. 3: Magnetic field distribution of inductance in the air gap and steel between the magnets.

As shown in Fig. 4, magnetic flux density in closed circuit, where steel has main effect on accuracy direction of magnetic flux.

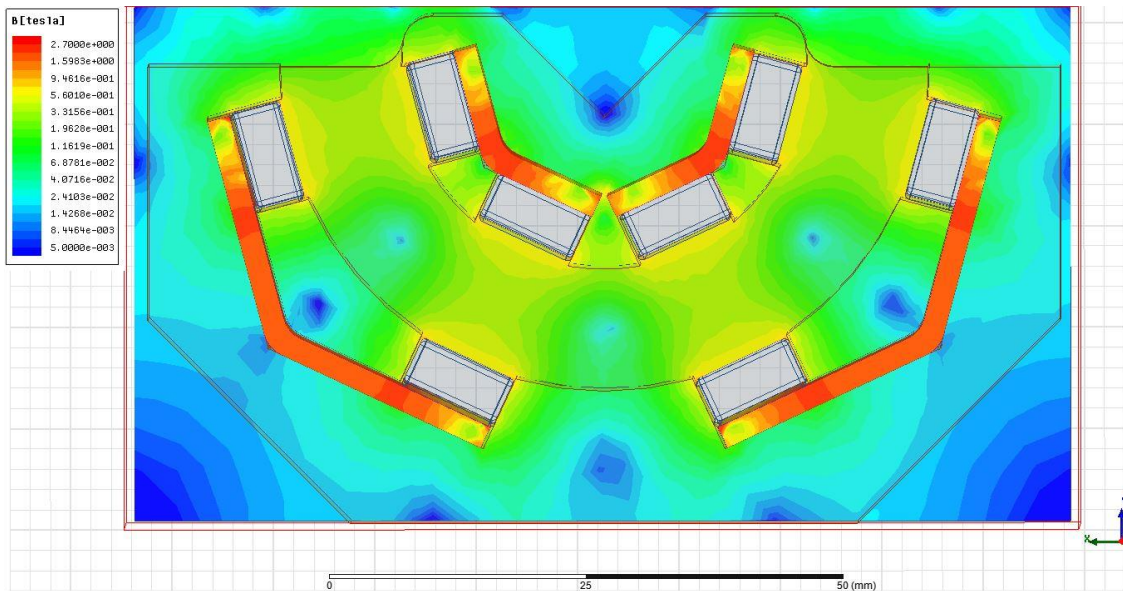


Fig. 4: Field distribution of magnetic flux density in the air gap and steel between the magnets.

As shown in Fig. 5, there are two sets of corridor track coils. The assembly is designed for easy handling and visual control during the measurement. Measurement was carried out both horizontally and vertically. Vertically compiled harvester as shown in Fig. 3a), have partially common phase. Fig. 3b), weight and coil in a phase.

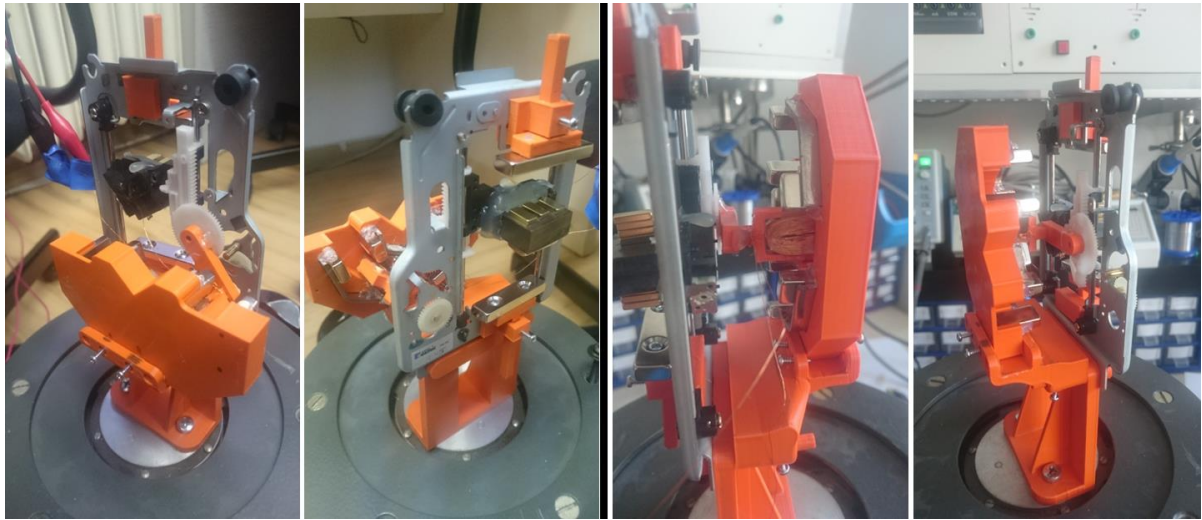


Fig. 5: a) Partially common phase;

Fig. 5: b) Common phase.

The third way of harvester assembly is horizontal, which is excited by oscillation sideways. Weight and coil are in the phase where earth gravity affect just the coil. Losses in the plastic rack, the pinion and total motion cause big losses to mechanism, which they will display outside of the weight and coil.

As shown in Fig. 6, captures a voltage at the resistance of $240\ \Omega$, excitation frequency 7 Hz and amplitude ± 2 , $U_{Pk-Pk} = 3.42\text{ V}$. Resistor has a lower value due to the simulation load. Asymmetric progress of generating voltage is caused by incomplete track of the coil between the magnets and their non - linear velocity in the given sections between the magnetic pairs. Fig. 7, captures a progress of a voltage at the resistance of $240\ \Omega$, excitation frequency 3 Hz and amplitude ± 3 , $U_{Pk-Pk} = 4.04\text{ V}$.

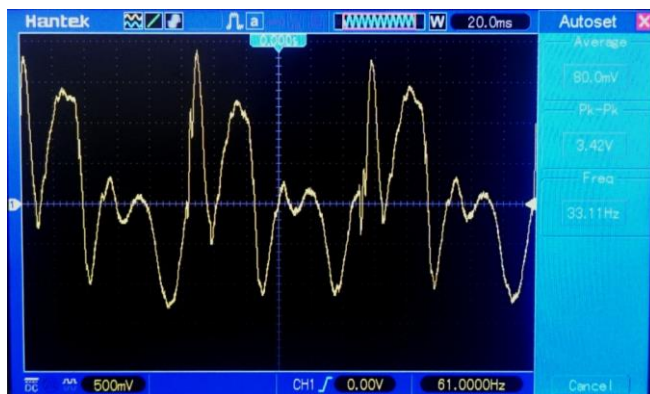


Fig. 6: The waveform of the voltage at 7 Hz.

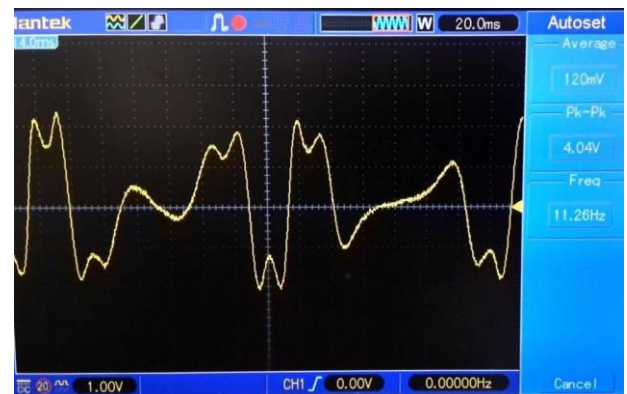


Fig. 7: The waveform of the voltage at 3 Hz.

3. Conclusion

This work studies design of a mechanical amplifier for low frequencies. The variety in the results creates a range of possibilities for optimization of the harvester. Measurements have shown the best results when keeping the dynamic parameters in a range of 3 – 8 Hz. To gain electric energy, however, excitation amplitude of $\pm 2\text{ mm}$ is necessary.

Acknowledgement

This work was supported by the grant from the Grant Agency of VEGA no. 1/0742/15 and by the Slovak Research and Development Agency under the contract no. APVV-15-0630.

References

- Sardini, E. and Serpelloni, M. (2011) An efficient electromagnetic power harvesting device for low-frequency applications. Sensors and Actuators A 172 pp. 475-482.
- Shahosseini, I. and Najafi, K. (2014) Mechanical Amplifier for Translational Kinetic Energy Harvester. Center for Wireless Integrated MicroSensing and Systems, University of Michigan, USA.